LANGMUIR

pubs.acs.org/Langmuir Article

Molecular Understanding of Ion Effect on Polyzwitterion Conformation in an Aqueous Environment

Yuan Xiang, Rong-Guang Xu, and Yongsheng Leng*

Cite This: https://dx.doi.org/10.1021/acs.langmuir.0c01287 Read Online

ACCESS | Metrics & More | Article Recommendations | Supporting Information

ABSTRACT: Polyzwitterions (PZs) are promising materials for the antifouling in reverse osmosis and nanofiltration membrane technology for water treatment. Fundamental understanding of the structure and molecular interactions involving zwitterions is crucial to the optimal design of antifouling in membrane separation. Here we employ the umbrella sampling and molecular dynamics simulations to investigate molecular interactions between sulfobetaine/carboxybetaine zwitterions and different metal ions (Na^+, K^+, and Ca^{2+}) in an aqueous solution. The simulation results show that these ions can form stable or metastable contact ionic/solvent-shared-ionic pairs with zwitterions. Simulations at different grafting densities of PZ brush arrays reveal complex competitive association mechanisms, which are attributed to nonbonded electrostatic and van der Waals interactions among zwitterions, water molecules, and different metal ions in an aqueous environment. While the high-grafting density of the PZ brush array leads to a strong branch association between different zwitterions in water, this association is decreased at intermediate- and low-grafting densities due to strong zwitterion−water interactions. More importantly, adding ions into water at intermediate- and low-grafting densities further breaks down the zwitterion branch association, resulting in a randomly oriented and dispersed branch configuration with significant swelling of the polymers. The degree of swelling depends on the type of ions, which further changes the surface electrostatic potential of PZ coatings.

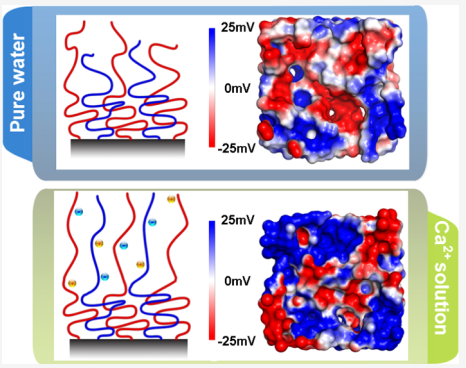

1. INTRODUCTION

Reverse osmosis and nanofiltration (RO/NF) membrane separation is considered to be a very promising technique to address the global portable water shortage.[1−3] However, membrane techniques also have their own deficiencies. One critical issue is related to the membrane fouling,[4,5] which is caused by accumulating foreign substances on the membrane surface, resulting in a substantial decline of membrane performance, such as reduced water flux and low effluent quality. In recent years, substantial efforts have been invested in the fundamental understanding of membrane fouling[6−12] and the development of relevant technologies. Among these, modifying the surface chemistry of the membrane, such as grafting antifouling monomers onto the membrane surface, has attracted much attention. It has been shown that this technique could be used to not only reduce surface fouling, but also improve the chlorine tolerance, salt rejection, and thermal stability of the RO/NF membranes.[13−17]

Poly(ethylene glycol) (PEG) and polyzwitterion (PZ) are two typical materials used for antifouling through the surface grafting technique.[18−20] They have the strong capability to bind water molecules, which is believed to be a key factor in antifouling applications. Compared with PEG coating, PZ coatings, such as poly(sulfobetaine) and poly(carboxybetaine), could be better candidates for antifouling materials due to their intriguing properties. The localized, opposite charge groups within a PZ chain could bind water molecules even stronger than a PEG chain molecule.[21] Further, PZ coatings are chemically more stable than PEG coating.[22] These two appealing properties make the PZ coatings very promising materials in antifouling applications. In addition to membrane technology application, they are now used in marine coating, drug delivery, and biomedical applications.[21,23−28]

To improve the antifouling performance of PZ coatings and to design next-generation antifouling materials, a fundamental understanding of the structural and molecular interactions involved in PZ coating is essential. Metal ions such as Na^+, K^+, and Ca^{2+} are ubiquitous in seawater desalination and wastewater reclamation processes. The effect of these ions on the structural properties of PZ coating is a fundamental question that needs to be answered. Further, the grafting density of PZ coatings on a membrane surface will also influence the surface structural and morphological properties. Understanding different pair interactions, including zwitter-

Received: May 1, 2020
Revised: June 5, 2020
Published: June 7, 2020

ion−zwitterion, zwitterion−ion, and zwitterion−water interactions, is crucial to the development of antifouling materials in membrane separations.

Experimental studies in this area have been focusing on grafting PZ coatings with a few rapid and low-cost methods,[29−31] such as chemical vapor deposition,[32] click chemistry,[33] and concentration-polarization-enhanced radical graft polymerization method.[34] Several computational molecular simulations also revealed the hydration behaviors of zwitterions and their interactions with different foulants.[35−39]

In this work, we perform molecular simulations to study two types of zwitterions, sulfobetaine and carboxybetaine, and investigate three fundamental aspects relevant to their hydration structure and antifouling properties: (1) using umbrella sampling to calculate free-energy profiles between zwitterion and different metal ions in aqueous solution (which are ubiquitous during seawater desalination and wastewater reclamation) to characterize their fundamental molecular interactions; (2) investigating the effect of grafting density on the hydration structure of zwitterion brush arrays; and (3) studying the ion effect on the swelling behavior, the so-called anti-polyelectrolyte property of the zwitterion brush array and its ion responsivity due to surface electrostatic potential changes. This work sheds new light on the molecular interactions between zwitterion coatings and their working environment, which is crucial for designing future antifouling materials.

2. MATERIALS AND METHODS

2.1. Molecular Models. *2.1.1. Polyzwitterion Model.* Zwitterions have two oppositely charged functional groups. In a sulfobetaine or carboxybetaine molecule, the sulfonate group ($-SO_3^-$) or the carboxylate group ($-COO^-$) carries a negative charge, while the quaternary ammonium group ($-N(CH_3)_3^+$) in both the molecules carries a positive charge (Figure 1a). PZ coatings on a polyamide membrane surface are modeled by the zwitterion brush arrays with different grafting densities (Figure 1b).[40] These sulfobetaine/carboxybetaine brush models are built based on the click chemistry method.[33] Details of building these brush models are described in Section S1, Supporting Information.

We consider short sulfobetaine or carboxybetaine brushes, with each brush containing five zwitterion branches (Figure 1c). Two saturated benzene rings are used to represent the root of the brush and the polyamide membrane, as shown in Figure 1b. We use the optimized potentials for liquid simulations (OPLSs) all-atom force field[41,42] to describe the interatomic interactions among zwitterions and between zwitterion and other species in aqueous solution. OPLS is well parameterized for most organic molecules and ions in aqueous solutions. Atomic partial charges in zwitterions are further recalibrated by quantum mechanical density functional theory calculations using B3LYP/6-31G** functional and basis set and by the CHarges from ELectrostatic Potentials using a Grid (CHELPG)-based method.[43] For two or three $-CH_2-$ spacer groups between oppositely charged groups in zwitterions, we find that recalibrated partial charges have only slight changes compared to OPLS charges, consistent with previous studies.[44] These recharacterized partial charges will be used in our simulations. Because of the different sizes among sulfonate ($-SO_3^-$), carboxylate ($-COO^-$), and quaternary ammonium ($-N(CH_3)_3^+$) groups, the charge densities of these groups are about −4.5, −5.3, and 3.0 e/nm^3, respectively, as shown in Figure 1a.

2.1.2. Aqueous Solution. The flexible simple point charge (SPC) water model[45,46] and Åqvist SPC-compatible ion potential parameters[47] for the Na^+, K^+, and Ca^{2+} ions are employed in our simulations. For halide Cl^- anion, we use the potential parameters developed by Joung et al.[48]

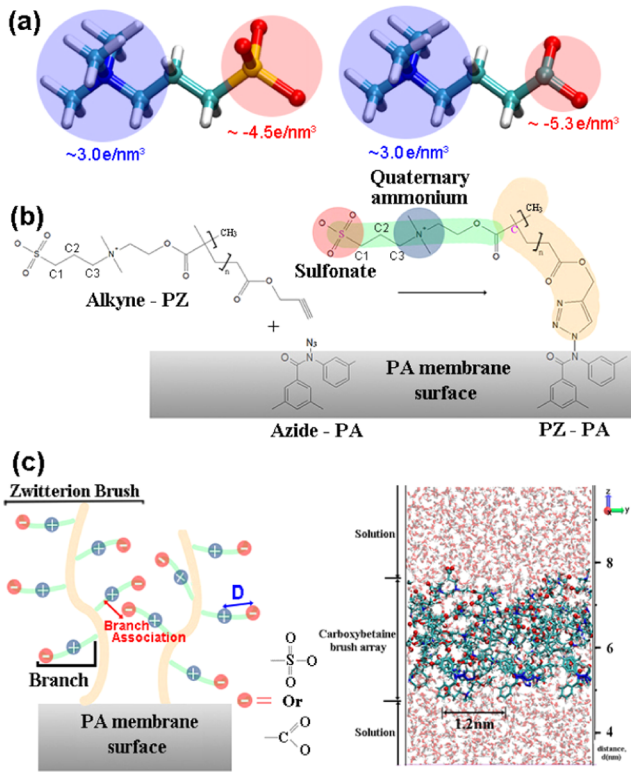

Figure 1. (a) Molecular structures of sulfobetaine (left) and carboxybetaine (right). Colors: red, O; white, H; light blue, C; dark blue, N; and yellow, S; charge densities of different zwitterion groups are shown in the figure; (b) click chemistry synthesize method of grafting sulfobetaine zwitterion onto a polyamide membrane surface. Three hydrocarbon $-CH_2-$ groups (indicated by C1−C3) are arranged between the sulfonate (red area) and quaternary ammonium groups (blue area); and (c) the structures of the zwitterion brushes. The definitions of the zwitterion brush and branch are illustrated in this panel. The branch association between the oppositely charged groups is shown by a red double arrow. The distance, *D*, shown in blue represents the distance between the quaternary ammonium C atoms and either sulfonate or carboxylate O atoms within the same zwitterion branch, which is beyond 5 Å. The right panel shows a snapshot of the carboxybetaine brush array with intermediate grafting density in water.

2.2. Simulation Methods. We use the LAMMPS computational package[49] to perform umbrella sampling and molecular dynamics (MD) simulations. In MD, periodic boundary conditions are applied in three dimensions. The particle−particle particle−mesh solver is used to calculate the long-range electrostatic interactions.[50] The cutoff distance for the short-range Lennard-Jones interactions is set to 10 Å. The equations of motion of the particles are propagated through the velocity Verlet algorithm with a time step of 1 fs in a constant-*NVT* ensemble. The temperature is controlled at 300 K using the Nosé−Hoover thermostat.[51]

The umbrella sampling method[52,53] is used for free-energy calculations between sulfobetaine/carboxybetaine molecules and three different metal ions, Na^+, K^+, and Ca^{2+}, which are balanced by Cl^- anions in aqueous solution. The detailed information about the umbrella sampling method is given in Section S2, Supporting Information.

For each sulfobetaine or carboxybetaine molecule, three independent MD simulation runs are performed at 300 K and 1 atm pressure in an *NPT* ensemble, in which one monovalent ion Na^+ or K^+ and one Cl^- anion or one divalent Ca^{2+} ion and two Cl^- anions are added to the simulation system. A total of 1600 water molecules are included in the system. In each case, a total of $N = 40$ succeeding

https://dx.doi.org/10.1021/acs.langmuir.0c01287
Langmuir XXXX, XXX, XXX−XXX

umbrella sampling intervals are arranged between d = 2 and 12 Å distance. A harmonic spring with a spring constant of 2 kcal/(mol Å^2) is used in the sampling. Molecular configurations are sampled by gradually changing the equilibrium distance of the spring within each sampling interval of 0.25 Å. The simulation time for each interval is 2 ns.

3. RESULTS

3.1. Free Energy between Zwitterion and Different Metal Ions in Water. Of the three fundamental interactions of zwitterion−zwitterion, zwitterion−ion, and zwitterion−water contact pairs, the second plays a major role in the disruption of zwitterion association in a salt solution.[54−58] Early studies have already investigated the zwitterion−ion association in water by calculating radial distribution functions, coordination numbers, and association lifetimes.[38] To provide a more fundamental understanding of this interaction, we use the umbrella sampling technique[52,53,59] to calculate free-energy changes versus the distance between the zwitterion molecules and different metal ions (Na^+, K^+, or Ca^{2+}) in water. Interactions between zwitterion quaternary ammonium groups and Cl^- anions are not further studied because of their nonspecific binding feature.[38]

The atomic distance, d, between metal ions and S atom in sulfobetaine or between metal ions and carboxylate C atom in carboxybetaine is used as a single collective variable for umbrella sampling (Figures 2a and S1c, the green dashed lines). Figure 2a−c shows free-energy variations versus the atomic distance d between sulfobetaine/carboxybetaine zwitterions and three different metal ions. To make a connection with previous simulation studies,[38] two $-CH_2-$ spacer groups are considered between the oppositely charged groups in a zwitterion. The free-energy value at larger distance d = 6.5 Å is used as the reference point. For zwitterion−Na^+ interaction (Figure 2a), the sulfobetaine profile exhibits a local minimum at about 3.9 Å, followed by a deeper and broader energy valley at 5.0−6.0 Å distance. The energy barrier between these two minima is around 1.33 kcal/mol, corresponding to the transition from the so-called contact ionic pair (CIP) to the solvent-shared ionic pair (SSIP) between the sulfonate and Na^+ ion (see the inset molecular configurations in Figure 2a, also see Figure S1a,b in the Supporting Information). The CIP configuration shows that one oxygen atom in the sulfonate group and five water molecules in the first hydration shell coordinate Na^+ ion to form a monodentate configuration. In the SSIP configuration, Na^+ ion has six water molecules in the first hydration shell, in which two of them also have an association with the sulfonate group. The SSIP configuration is energetically more favorable than the CIP configuration, with a further free energy decrease by about 0.95 kcal/mol. Dissociation of this SSIP requires overcoming a second energy barrier of 1.41 kcal/mol at 5.9−6.5 Å distance, as shown in Figure 2a.

Compared with sulfobetaine−Na^+ association, Figure 2a shows that the carboxybetaine−Na^+ association has a much lower free energy at CIP configuration than at SSIP configuration. These two configurations are shown in Figure S1c,d, suggesting that CIP is more energetically favorable than SSIP by 0.49 kcal/mol. The energy barrier for SSIP dissociation is about 1.60 kcal/mol, slightly higher than that of sulfobetaine−Na^+ dissociation.

In Figure 2b, the sulfobetaine−K^+ interaction has similar free energies at CIP and SSIP configurations and the energy barrier between them is only about 0.59 kcal/mol. This energy barrier is comparable to the ambient thermal energy k_BT (~0.6 kcal/mol), indicating that the transition between CIP and SSIP could be easily proceeded at room temperature. For the carboxybetaine−K^+ interaction, the free energy of SSIP is further lower than that of its CIP configuration, indicating that SSIP is more energetically favorable. The overall less barriers for the CIP → SSIP transition and the SSIP dissociation of zwitterion−K^+ interaction, compared to zwitterion−Na^+ interaction, are attributed to the relatively lower hydration energy of K^+ (−64.5 kcal/mol) than that of Na^+ (−94.8 kcal/mol).[60] The CIP and SSIP configurations of zwitterion−K^+ ion are shown in Figure S1e−h. Interestingly, in the CIP configurations, both sulfonate and carboxylate groups largely adopt the so-called bidentate configuration with K^+ ion (Figure S1e,g), in which two oxygen atoms from the sulfonate or carboxylate group equally coordinate K^+ ion in its first

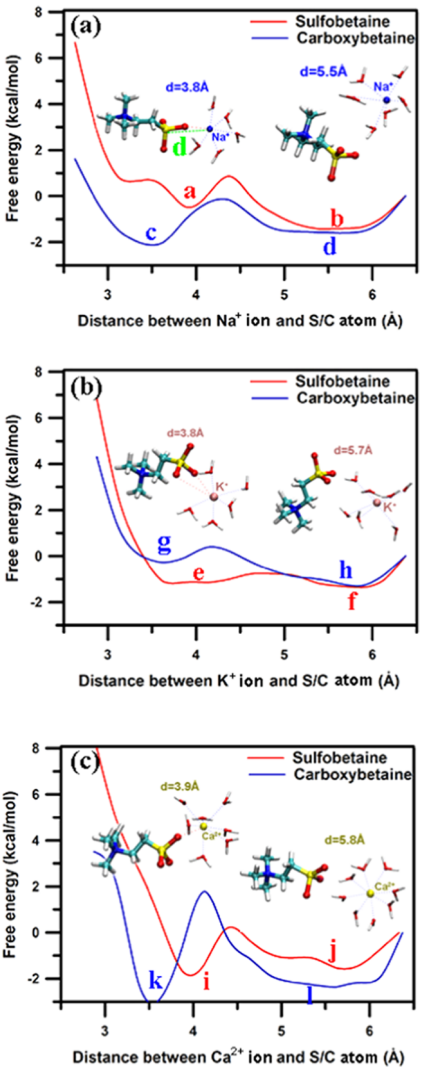

Figure 2. Variations of the free energy versus the atomic distance, d, between zwitterions (sulfobetaine or carboxybetaine) and (a) Na^+; (b) K^+; and (c) Ca^{2+} ions in a salt solution. The atomic distance, d, is defined as the distance between the metal ion and the S atom in the sulfobetaine or the C atom in the carboxybetaine zwitterion. The insets show typical binding structures between sulfobetaine and metal ions. Point a−l correspond to the CIP or SSIP configurations, as shown in Figure S1a−l, respectively.

https://dx.doi.org/10.1021/acs.langmuir.0c01287
Langmuir XXXX, XXX, XXX−XXX

hydration shell. These two oxygen atoms, together with other five water molecules, form the first hydration shell of K^+ ion in aqueous solution, consistent with other studies.[61−63]

In Figure 2c, both sulfobetaine and carboxybetaine show a very strong CIP binding than their SSIP binding with Ca^{2+} divalent ion. The CIP → SSIP transition barriers are also higher than other cases of monovalent ion binding. These energy barriers are 1.97 and 4.66 kcal/mol for sulfobetaine− and carboxybetaine−Ca^{2+} interactions, respectively. Molecular configurations of CIP and SSIP configurations are shown in Figure S1i−l. Similar to the interactions with Na^+ ion, monodentate configuration is dominant in CIP configuration, in which one oxygen atom from the sulfonate or carboxylate group replaces one of the eight hydration water molecules in the first hydration shell of Ca^{2+}. Dissociation barriers of SSIPs for the sulfonate− and carboxylate−Ca^{2+} interactions are 1.54 and 2.36 kcal/mol, respectively. These very high energy barriers, as expected, are due to the much higher hydration energy of Ca^{2+} ion (−311 kcal/mol) than those of monovalent ions (Na^+ and K^+).[60]

Our free-energy simulation results discussed above could reveal the mechanism of previous studies, which showed that the association lifetime for the carboxybetaine−Na^+ pair is longer than the sulfobetaine−Na^+ pair, while the association lifetime of carboxybetaine−K^+ is slightly shorter than the sulfobetaine−K^+ pair.[38] Moreover, it is shown that even for the same functional group but in different material environments, the binding with the same metal ions exhibits different behaviors in aqueous solution. For example, in our previous studies, we reported that the carboxylate group in polyamide prefers to form a bidentate CIP configuration with Ca^{2+} ions in aqueous solution.[64,65] Here, the carboxylate group in carboxybetaine tends to form only monodentate configuration with Ca^{2+} ions.

3.2. Polyzwitterion Association in Water and in $CaCl_2$ Salt Solution. Three grafting densities of the zwitterion brush (Figure 1b) are considered to investigate zwitterion branch associations. The relevant low-, intermediate-, and high-density definitions of the grafting of PZ coatings on a polyamide membrane surface simulation systems are given in Table 1.

Table 1. Three Grafting Densities of the Zwitterion Brush Arrays Used in Simulations

	number of zwitterion brushes	area per brush (nm^2)	distance between brushes (nm)
low density	9	3.24	1.8
intermediate density	9	1.44	1.2
high density	16	0.64	0.8

These grafting density numbers correspond to the material volume density estimates based on Fourier transform infrared (FTIR) spectra measurements (~1 g/cm^3), assuming that the coating thickness is around a few micrometers in the experiment.[33] As will be seen later in Figure S3, the intermediate- and high-grafting densities in our simulations correspond to 0.74 and 1.6 g/cm^3.

The procedure of building the zwitterion brush array is described in Section S1, Supporting Information. When studying the branch association in NaCl/KCl/$CaCl_2$ solution, 45 $Na^+/K^+/Ca^{2+}$ ions and balanced Cl^- ions are added to the system, resulting in a 0.3 M salt solution. A total of 2 ns equilibrium run is performed for each system, followed by data collection and configuration analysis.

Figure S2 shows typical molecular configurations of the hydrated carboxybetaine brush arrays in water at three grafting densities (for the intermediate grafting density, see also Figure 1c). In general, both sulfobetaine and carboxybetaine brush arrays exhibit vertically aligned self-assembled structures at a high grafting density, while at intermediate and low grafting densities, they tend to be more randomly oriented. To quantify the degree of association among zwitterion branches, we calculate the coordination number of each O atom in either sulfonate or carboxylate groups surrounded by C atoms in the quaternary ammonium groups, within a distance of 3.5 Å. This is because upon a zwitterion association, the distance between the quaternary ammonium C and the sulfonate/carboxylate O atoms between two different zwitterions is well within the range of 3−3.5 Å (see the red arrow in Figure 1c), much smaller than the corresponding distance between the relevant atoms in the same zwitterion branch, which is larger than 5 Å (see the blue arrow in Figure 1c).

As we find that the divalent Ca^{2+} ion in $CaCl_2$ solution has a significant effect on zwitterion association compared to Na^+ and K^+ ions in NaCl and KCl solutions, in the following discussion we focus on a comparative study on the zwitterion association in water and in $CaCl_2$ solutions. Figure 3 shows

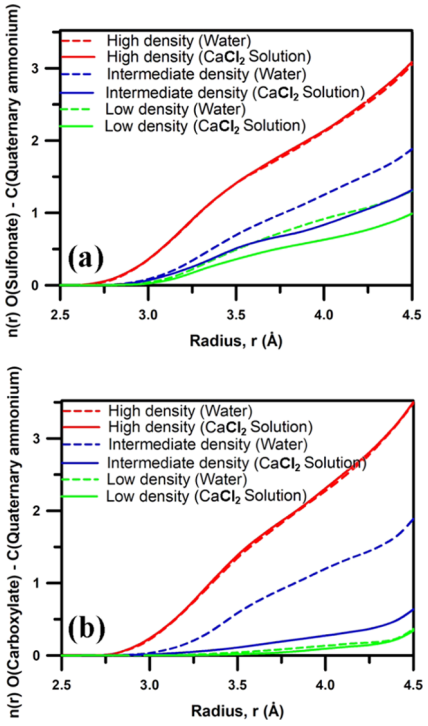

Figure 3. Coordination numbers between (a) oxygen atoms in sulfonate and carbon atoms in quaternary ammonium and (b) oxygen atoms in carboxylate and carbon atoms in quaternary ammonium, in water and $CaCl_2$ solution at different grafting densities.

variations of the C coordination number around each O atom in sulfobetaine/carboxybetaine in both water and $CaCl_2$ solutions. In Figure 3a, the degree of sulfobetaine branch association is seen to increase with the grafting density. For instance, at 3.5 Å distance in water, only 0.50 quaternary ammonium C atom is associated with a sulfonate O atom in the low-grafting-density array, while in the high-grafting-

https://dx.doi.org/10.1021/acs.langmuir.0c01287
Langmuir XXXX, XXX, XXX−XXX

density array, this coordination number is increased to 1.42. Figure 3b shows that the carboxybetaine association in water is also higher in the high-grafting-density array than in the low-grafting-density array. This dependence of zwitterion association on the grafting density is attributed to the hydration state, as discussed in our previous studies.[40] We find that both sulfonate and carboxylate groups in a high-grafting-density state are less hydrated than in a low-grafting-density state. In such a scenario, the dissociation energy between two zwitterion branches is much higher than that in a fully hydrated state,[40] resulting in a strong branch association. Figure 3b shows that in the low-grafting-density state, the zwitterion association of carboxybetaine is even weaker, as the relevant C coordination number around each O atom of the carboxylate group in water is only about 0.05 at the 3.5 Å distance, much smaller than that of sulfobetaine due to the larger hydration energy of the carboxylate group.[38]

In $CaCl_2$ solution, Figure 3a,b shows that in the high-grafting-density state, the ion effect of Ca^{2+} on the zwitterion association is almost negligible. In the intermediate-grafting-density state, sulfobetaine has a mild decrease of branch association compared with in pure water, while carboxybetaine exhibits a dramatic decline in branch association. In the low-grafting-density state, sulfobetaine still has a moderate decline in branch association, while carboxybetaine has almost no change.

To visualize and understand the particular zwitterion dissociation in water and in $CaCl_2$ solution in the intermediate-grafting-density state, in Figure 4, we show molecular conformation changes of the sulfobetaine and carboxybetaine brush arrays in water and in $CaCl_2$ solution. Figure 4a,b shows the top views of the zwitterion brush arrays in water with a moderate association. Representative local aggregations of branches are highlighted with purple circles. The degree of association can be quantified by the surface coverage of zwitterions. A higher degree of branch association corresponds to a lower surface coverage, defined as the ratio of the projection of the van der Waals branch surface to the area of horizontal plane of the simulation box. In pure water, we find that the surface coverages of the two types of zwitterion branches are all around 70%. Figure 4c shows the equilibrium conformation of sulfobetaine branches in $CaCl_2$ solution. Ca^{2+} ions (yellow balls in the figure) form either CIP or SSIP with the sulfonate groups, resulting in some dissociation of sulfobetaine aggregations, as evidenced by the increased surface coverage from 70 to about 81%. For carboxybetaine, Figure 4d shows more significant branch dissociation in $CaCl_2$ solution, corresponding to a more randomly oriented and dispersed phase. The surface coverage of carboxybetaine is increased from 70% in water to 90% in $CaCl_2$ solution. This is consistent with the larger decline in the O−C coordination number in carboxybetaine than in sulfobetaine in $CaCl_2$ solution (Figure 3). According to our calculations, 24 ± 5 out of a total of 45 Ca^{2+} ions are associated with the sulfonate groups through either CIP or SSIP configurations. This associated ion number is increased to 35 ± 6 Ca^{2+} ions for the carboxylate groups, indicating that Ca^{2+} ion has a much stronger interaction with carboxybetaine than with sulfobetaine, consistent with previous free-energy calculations (Figure 2c).

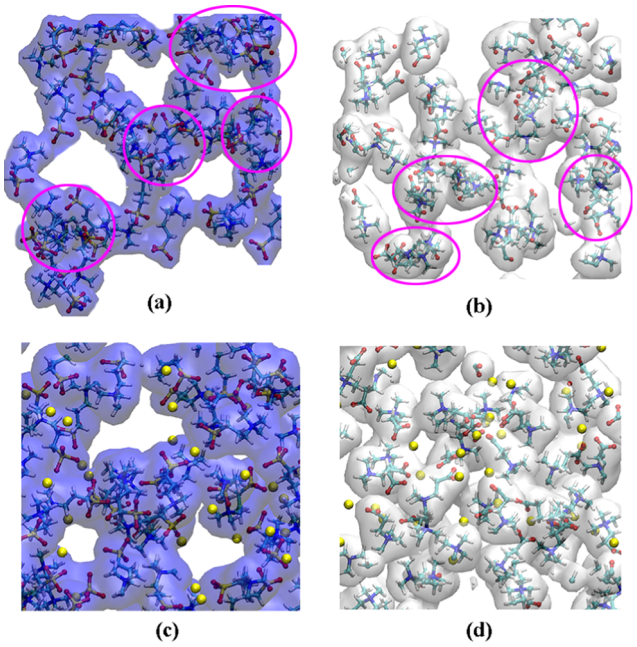

Figure 4. Top-view snapshots at the intermediate grafting density of (a) sulfobetaine branches in water; (b) carboxybetaine branches in water; (c) sulfobetaine branches in $CaCl_2$ solution; and (d) carboxybetaine branches in $CaCl_2$ solution. The blue and white surfaces represent van der Waals contours of sulfobetaine and carboxybetaine branches, respectively, which are used to estimate the surface coverages. The typical branch association is marked by the purple circles in Panels (a) and (b). Colors: red, O; white, H; light blue, C; dark blue, N; and yellow, S. Ca^{2+} ions are represented by the yellow balls.

It is worth noting that the probability of Ca^{2+} cations simultaneously associating with multiple zwitterion branches gradually increases from low to high grafting density, giving 8, 10, and 12%, respectively. These numbers are higher than those of monovalent ions (Na^+ or K^+) that can simultaneously associate with multiple zwitterion branches, which vary from 3 to 5% at low to high grafting densities. To summarize, at intermediate grafting density, strong zwitterion−ion interactions disrupt the zwitterion association, resulting in a more dispersed phase in salt solutions.

It is somewhat surprising that for carboxybetaine with a low grafting density, adding ions has almost no effect on zwitterion association (Figure 3b). This is because carboxybetaine branches are already fully hydrated and there is almost no branch association in water. When Ca^{2+} ions are present, the formation of CIP or SSIP with the carboxylate groups in the salt solution has almost no effect on the further zwitterion dissociation. In contrast, sulfobetaine tends to keep branch association even at a low grafting density (Figure 3a), and Ca^{2+} ions certainly play a role in further dissociating the zwitterion brushes.

Our simulation results could explain a recent experimental finding that sulfobetaine hydrogels have a much smaller equilibrium water content than that of carboxybetaine in the fully swollen state.[66]

3.3. Anti-polyelectrolyte Behavior and Surface Electrostatic Potentials of Polyzwitterion Arrays. The ion-induced zwitterion dissociation increases the thickness of the PZ brush arrays. This polymer swelling phenomenon, the so-called "anti-polyelectrolyte" behavior, has been reported by several researchers.[67−70] In pure water, the PZ brushes are usually in a relatively collapsed state due to zwitterion

https://dx.doi.org/10.1021/acs.langmuir.0c01287
Langmuir XXXX, XXX, XXX−XXX

association. However, upon increasing the ionic strength of the solution, the PZ brushes adopt a more expanded conformation due to the screening effect of the electrostatic interactions among them. This anti-polyelectrolyte behavior is seen to be the most pronounced for the intermediate-grafting-density brush arrays, as discussed previously.

In Figure S3a,b, we show the density distributions of the sulfobetaine and carboxybetaine brush arrays at intermediate grafting density in water and in $CaCl_2$ solution. If we define the water−PZ boundary as the distance at which the density of water molecules is about 80% of its bulk value (1 g/cm^3), then we find that the thicknesses of the sulfobetaine arrays in water and in $CaCl_2$ solution are 2.27 and 2.50 nm, respectively (marked by the red and black horizontal arrows in Figure S3a), yielding material densities of 0.738 and 0.673 g/cm^3, in the two different solutions for this PZ coating. The carboxybetaine brush arrays in water and in $CaCl_2$ solution share very similar values (Figure S3b). In Figure S3a,b, we also show the density distributions of Ca^{2+} and Cl^- ions within the PZ coating and in $CaCl_2$ solution. These density distributions exhibit no significant difference in different regions.

For comparison, in Figure S3c,d, we plot the same material density distributions at the high grafting density of the PZ arrays. It is seen that zwitterion densities in water and in $CaCl_2$ solution are almost indistinguishable, while those of Ca^{2+} and Cl^- are mainly located outside the PZ coating. This is because at high grafting density of the zwitterion brush array, it is rather difficult for both water molecules and different ions to penetrate into the dense PZ coating due to geometric constraints and strong zwitterion association. This phenomenon also explains why Ca^{2+} ions have almost no effect on O−C coordination numbers shown in Figure 3a,b (red lines) at this high grafting density.

The material density distributions shown in Figure S3 can explain some ion effects on the swelling of zwitterion coatings observed in experiments. In general, the density of a zwitterion coating on a substrate is inhomogeneous in the vertical thickness direction due to the following two reasons, as illustrated in Figure 5a,b: (1) the lengths of the zwitterion brushes are different as the molecular weight of each brush is difficult to be precisely controlled in experiments and (2) some brushes have more twisted conformations than others. Thus, the whole region of a PZ coating could be broadly divided into two subregions: the dense confined layer near the substrate and the relatively loose diffuse layer far from the substrate. As the ion effect on swelling behavior depends on the polymer density (Figures 3 and S3), different regions will have different hydration behaviors. The schematics of the ion effect on the conformation of a PZ coating in an electrolyte solution is illustrated in Figure 5c,d. In the dense layer, the internal branch association is dominant, preventing the hydrated salt ions from permeation into the dense layer. In contrast, the ions can easily access the loose diffuse layer far from the substrate, resulting in significant polymer swelling due to ion-induced branch dissociation. The implication of our simulation is that these results can explain the multiple-region structure of zwitterion coating and different hydration behaviors in different regions in salt solution, which are observed in recent neutron reflectivity[69] and spectroscopic ellipsometry experiments.[70]

Figure 6 shows the effect of electrolyte solution on the swelling degree of the zwitterion brush arrays, defined as the percent increase of PZ thickness relative to the one in pure water. As shown in the figure, the swelling degree of the zwitterion brush arrays at intermediate and low grafting densities depends on the type of ions present in aqueous solutions, as observed in previous experimental studies.[68,71] The swelling degree varies from 5 to 10.5% for both sulfobetaine and carboxybetaine at the two grafting densities. As expected, the carboxybetaine brush array has the highest swelling degree in $CaCl_2$ solution. These results, however, are somewhat less than the experimental results from spectroscopic ellipsometry measurements,[68] which is typically about several tens percent. The reason is that we only consider the ion-induced dissociation between different brushes (the green arrow shown in Figure 5c) due to the short brush models used in our simulations. In fact, ion-induced dissociation could also happen within the same brush if it is long enough and heavily twisted (the purple arrow shown in Figure 5c). The latter may lead to more significant swelling. In 0.3 M electrolyte solutions, the order of swelling degree for the sulfobetaine brushes is $Na^+ < K^+ < Ca^{2+}$, which follows the Hofmeister series[68,72] and is in good agreement with the spectroscopic ellipsometry measure-

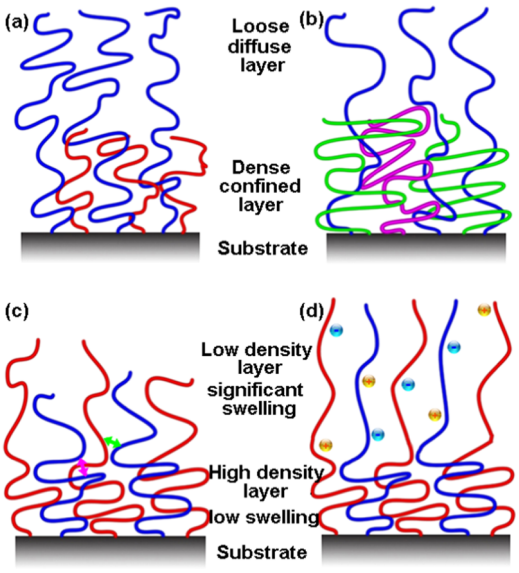

Figure 5. Schematics of the origin of the inhomogeneous density distribution of PZ coatings in the vertical thickness direction due to (a) different brush lengths and (b) some brushes having more twisted conformations than others. Panels (c) and (d) illustrate different coating conformations in water and in salt solution, respectively. The yellow and blue balls in (d) represent ions and anions in aqueous solution. The green arrow in (c) indicates the association between different brushes, and the purple arrow shows the self-association within the same brush. For clarity, the detailed conformation of branches in each brush is not shown in the panels.

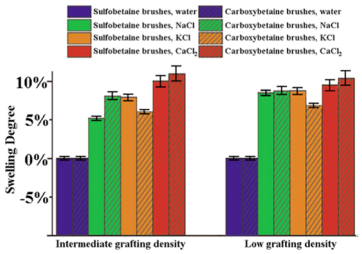

Figure 6. Swelling degrees of sulfobetaine and carboxybetaine brush arrays in water (defined as zero) and in different electrolyte solutions at intermediate and low grafting densities.

https://dx.doi.org/10.1021/acs.langmuir.0c01287
Langmuir XXXX, XXX, XXX−XXX

ments.[68] For the carboxybetaine brushes, however, the order of swelling degree is $K^+ < Na^+ < Ca^{2+}$, which does not comply with the Hofmeister series but is consistent with the free-energy profiles shown in Figure 2. This figure suggests that the CIP configuration is more favorable for carboxybetaine−Na^+ and carboxybetaine−Ca^{2+} binding than carboxybetaine−K^+ binding. Therefore, the free energy of zwitterion−ion interaction could be another indicator to characterize the ion-induced brush dissociation and the swelling of PZ coatings.

The ion effect on the swelling of PZ coating also changes the surface electrostatic potential, a character of its membrane ion responsivity.[73] This phenomenon is particularly significant for the carboxybetaine brush array in $CaCl_2$ solution. Figure 7

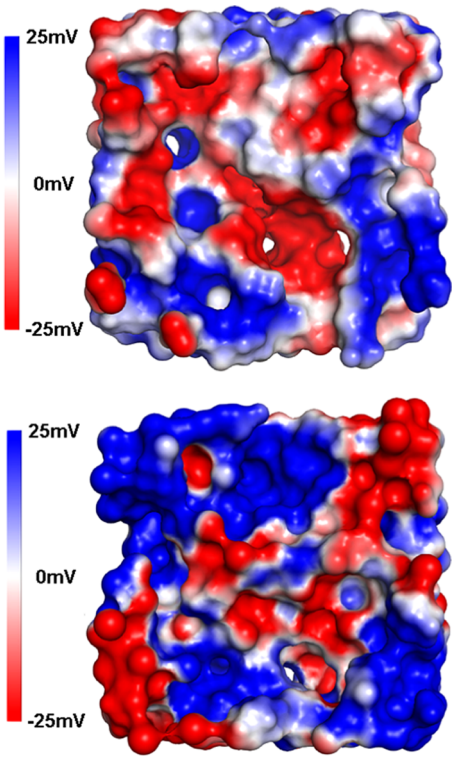

Figure 7. Surface electrostatic potential distributions of the carboxybetaine brush array (represented by a van der Waals surface) at intermediate grafting density in (a) water and (b) 0.3 M $CaCl_2$ solution.

shows the surface electrostatic potential distributions of the carboxybetaine brush array (represented by the van der Waals surface) in pure water and in 0.3 M $CaCl_2$ solution at an intermediate grafting density. These potentials are calculated by averaging over 2 ns MD equilibrium runs. The blue region shows the positive surface potential and the red region shows the negative surface potential distributions. In water, the area of the positive potential region is roughly equal to that of the negative potential region. The total average of the surface potential of the whole area is 0 ± 3 mV, signifying a neutral surface. In $CaCl_2$ solution, however, the positive potential region is increased significantly, accompanied by the reduction of the negative region. The total average of the surface potential is increased to 16 ± 5 mV. Although the change of the PZ surface electrostatic potential in electrolyte aqueous solutions was reported in experiments,[73] there is no consensus of the underline mechanisms due to the complex electrostatic interactions among electrolytes, water, and different charge groups in the zwitterion brushes. Our simulation results suggest that the strong carboxylate−Ca^{2+} binding and the nonspecific quaternary ammonium−Cl^- binding due to the large size and thus low charge density of the quaternary ammonium group (Figure 1a) could explain the increased surface electrostatic potential of the carboxybetaine brush array in $CaCl_2$ solution. More specifically, the dominant binding configurations of carboxylate−Ca^{2+} CIPs and much dispersed Cl^- anions in PZ coating result in more Ca^{2+} ions present in the zwitterion brush array, compared to less Cl^- anions existing in the same region, which makes the PZ coating positively charged on its surface. According to our calculations, we find that on average, there are about 93% of all Ca^{2+} ions located in the PZ array, whereas about 89% of all Cl^- anions present in the same brush array. Consequently, such a PZ coating should be considered as a responsive layer, for which the surface morphology, hydration behavior, and surface electrostatic potential could be controlled by the ions in electrolyte solutions.

4. CONCLUSIONS

The present study provides a further molecular understanding of the hydration behavior of zwitterion coatings on membrane surfaces. Polyzwitterions are promising antifouling materials in reverse osmosis and nanofiltration membrane technology for water treatment. However, the detailed molecular structure properties of zwitterion coatings and their interaction with different species in the aqueous environment have not yet been fully understood. We investigate through umbrella sampling and MD simulations the interactions between sulfobetaine/carboxybetaine zwitterions and three different metal ions (Na^+, K^+, and Ca^{2+}), as well as the ion effect on the overall hydration structure of different PZ coatings at different grafting densities. The simulation results show that carboxybetaine is more energetically favorable to form the CIP configuration with Na^+ and Ca^{2+} and the SSIP configuration with K^+, whereas sulfobetaine is more favorable to form the SSIP configuration with Na^+ and the CIP configuration with Ca^{2+}. More specifically, at the intermediate grafting density, Ca^{2+} ions in a $CaCl_2$ solution can further break down zwitterion branch associations, resulting in the swelling of PZ polymer coatings. The swelling degree can reach as high as 10.5% for both sulfobetaine and carboxybetaine brush arrays. Additionally, ion effect also changes the surface electrostatic potential of PZ coatings, from almost neutral in water to a positive surface potential in $CaCl_2$ electrolyte solution.

The present work provides valuable information on the interactions involving zwitterion coatings in relevant environmental and industry implementations, benefiting the molecular design of antifouling materials. For instance, when designing a zwitterion coating, one should prevent zwitterion materials from grafting into membrane pore surfaces, as the swelling of the zwitterion material in the moderate ionic strength solutions will induce a significant flux decline of the membrane.[74] Moreover, pretreatment of feed solutions containing high concentrations of divalent metal ions is important before applying PZ coatings. This is because these divalent ions will change the surface electrostatic potential of PZ coatings, leading to the deterioration of their antifouling performance against negatively charged foulants,[75] such as alginate and humic acid molecules.

https://dx.doi.org/10.1021/acs.langmuir.0c01287
Langmuir XXXX, XXX, XXX−XXX

■ ASSOCIATED CONTENT

Supporting Information

The Supporting Information is available free of charge at https://pubs.acs.org/doi/10.1021/acs.langmuir.0c01287.

Methods of building polyzwitterion model (Section S1) and umbrella sampling (Section S2); detailed binding structures between zwitterions and different metal ions in aqueous solution (Figure S1); snapshots of the carboxybetaine brush arrays with three different grafting densities in water (Figure S2); and density distributions of the zwitterion brush arrays in water and in $CaCl_2$ solution (Figure S3) (PDF)

■ AUTHOR INFORMATION

Corresponding Author

Yongsheng Leng − *Department of Mechanical & Aerospace Engineering, The George Washington University, Washington, District of Columbia 20052, United States;* orcid.org/0000-0002-3558-5016; Phone: 202-994-5964; Email: leng@gwu.edu

Authors

Yuan Xiang − *Department of Mechanical & Aerospace Engineering, The George Washington University, Washington, District of Columbia 20052, United States;* orcid.org/0000-0002-4665-3360

Rong-Guang Xu − *Department of Mechanical & Aerospace Engineering, The George Washington University, Washington, District of Columbia 20052, United States*

Complete contact information is available at: https://pubs.acs.org/10.1021/acs.langmuir.0c01287

Notes

The authors declare no competing financial interest.

■ ACKNOWLEDGMENTS

This work was supported by the National Science Foundation (NSF 1817394) and the resources of the National Energy Research Scientific Computing Center, a DOE Office of Science User Facility supported by the Office of Science of the U.S. Department of Energy under Contract no. DE-AC02-05CH11231.

■ REFERENCES

(1) Elimelech, M.; Phillip, W. A. The future of seawater desalination: Energy, technology, and the environment. *Science* **2011**, *333*, 712−717.

(2) Zhao, S.; Zou, L.; Tang, C. Y.; Mulcahy, D. Recent developments in forward osmosis: Opportunities and challenges. *J. Membr. Sci.* **2012**, *396*, 1−21.

(3) Greenlee, L. F.; Lawler, D. F.; Freeman, B. D.; Marrot, B.; Moulin, P. Reverse osmosis desalination: Water sources, technology, and today's challenges. *Water Res.* **2009**, *43*, 2317−2348.

(4) Lee, K. P.; Arnot, T. C.; Mattia, D. A review of reverse osmosis membrane materials for desalination-development to date and future potential. *J. Membr. Sci.* **2011**, *370*, 1−22.

(5) Tang, C. Y.; Chong, T. H.; Fane, A. G. Colloidal interactions and fouling of nf and ro membranes: A review. *Adv. Colloid Interface Sci.* **2011**, *164*, 126−143.

(6) Eslami, H.; Muller-Plathe, F. Molecular dynamics simulation of water influence on local structure of nanoconfined polyamide-6,6. *J. Phys. Chem. B* **2011**, *115*, 9720−9731.

(7) Harder, E.; Walters, D. E.; Bodnar, Y. D.; Faibish, R. S.; Roux, B. Molecular dynamics study of a polymeric reverse osmosis membrane. *J. Phys. Chem. B* **2009**, *113*, 10177−10182.

(8) Hughes, Z. E.; Gale, J. D. A computational investigation of the properties of a reverse osmosis membrane. *J. Mater. Chem.* **2010**, *20*, 7788−7799.

(9) Kotelyanskii, M.; Wagner, N. J.; Paulaitis, M. E. Building large amorphous polymer structures: Atomistic simulation of glassy polystyrene. *Macromolecules* **1996**, *29*, 8497−8506.

(10) Nadler, R.; Srebnik, S. Molecular simulation of polyamide synthesis by interfacial polymerization. *J. Membr. Sci.* **2008**, *315*, 100−105.

(11) Ridgway, H. F.; Orbell, J.; Gray, S. Molecular simulations of polyamide membrane materials used in desalination and water reuse applications: Recent developments and future prospects. *J. Membr. Sci.* **2017**, *524*, 436−448.

(12) Wei, T.; Zhang, L.; Zhao, H. Y.; Ma, H.; Sajib, M. S. J.; Jiang, H.; Murad, S. Aromatic polyamide reverse-osmosis membrane: An atomistic molecular dynamics simulation. *J. Phys. Chem. B* **2016**, *120*, 10311−10318.

(13) Rana, D.; Matsuura, T. Surface modifications for antifouling membranes. *Chem. Rev.* **2010**, *110*, 2448−2471.

(14) Li, D.; Wang, H. Recent developments in reverse osmosis desalination membranes. *J. Mater. Chem.* **2010**, *20*, 4551−4566.

(15) Perreault, F.; Tousley, M. E.; Elimelech, M. Thin-film composite polyamide membranes functionalized with biocidal graphene oxide nanosheets. *Environ. Sci. Technol. Lett.* **2014**, *1*, 71−76.

(16) Bai, L. M.; Liu, Y. T.; Bossa, N.; Ding, A.; Ren, N. Q.; Li, G. B.; Liang, H.; Wiesner, M. R. Incorporation of cellulose nanocrystals (cncs) into the polyamide layer of thin-film composite (TFC) nanofiltration membranes for enhanced separation performance and antifouling properties. *Environ. Sci. Technol.* **2018**, *52*, 11178−11187.

(17) Hao, X. J.; Gao, S. S.; Tian, J. Y.; Sun, Y.; Cui, F. Y.; Tang, C. Y. Y. Calcium-carboxyl intrabridging during interfacial polymerization: A novel strategy to improve antifouling performance of thin film composite membranes. *Environ. Sci. Technol.* **2019**, *53*, 4371−4379.

(18) Vaisocherová, H.; Yang, W.; Zhang, Z.; Cao, Z. Q.; Cheng, G.; Piliarik, M.; Homola, J.; Jiang, S. Y. Ultralow fouling and functionalizable surface chemistry based on a zwitterionic polymer enabling sensitive and specific protein detection in undiluted blood plasma. *Anal. Chem.* **2008**, *80*, 7894−7901.

(19) Yang, W.; Chen, S. F.; Cheng, G.; Vaisocherova, H.; Xue, H.; Li, W.; Zhang, J. L.; Jiang, S. Y. Film thickness dependence of protein adsorption from blood serum and plasma onto poly(sulfobetaine)-grafted surfaces. *Langmuir* **2008**, *24*, 9211−9214.

(20) Zhang, Z.; Chao, T.; Chen, S.; Jiang, S. Superlow fouling sulfobetaine and carboxybetaine polymers on glass slides. *Langmuir* **2006**, *22*, 10072−10077.

(21) Jiang, S.; Cao, Z. Ultralow-fouling, functionalizable, and hydrolyzable zwitterionic materials and their derivatives for biological applications. *Adv. Mater.* **2010**, *22*, 920−932.

(22) Gaberc-Porekar, V.; Zore, I.; Podobnik, B.; Menart, V. Obstacles and pitfalls in the pegylation of therapeutic proteins. *Curr. Opin. Drug Discovery Dev.* **2008**, *11*, 242−250.

(23) Chang, Y.; Chang, W. J.; Shih, Y. J.; Wei, T. C.; Hsiue, G. H. Zwitterionic sulfobetaine-grafted poly(vinylidene fluoride) membrane with highly effective blood compatibility via atmospheric plasma-induced surface copolymerization. *ACS Appl. Mater. Interfaces* **2011**, *3*, 1228−1237.

(24) Chen, S. F.; Zheng, J.; Li, L. Y.; Jiang, S. Y. Strong resistance of phosphorylcholine self-assembled monolayers to protein adsorption: Insights into nonfouling properties of zwitterionic materials. *J. Am. Chem. Soc.* **2005**, *127*, 14473−14478.

(25) Schlenoff, J. B. Zwitteration: Coating surfaces with zwitterionic functionality to reduce nonspecific adsorption. *Langmuir* **2014**, *30*, 9625−9636.

(26) Yang, W. J.; Neoh, K. G.; Kang, E. T.; Teo, S. L. M.; Rittschof, D. Polymer brush coatings for combating marine biofouling. *Prog. Polym. Sci.* **2014**, *39*, 1017−1042.
(27) Koc, J.; Schonemann, E.; Arnuthalingam, A.; Clarke, J.; Finlay, J. A.; Clare, A. S.; Laschewsky, A.; Rosenhahn, A. Low-fouling thin hydrogel coatings made of photo-cross-linked polyzwitterions. *Langmuir* **2019**, *35*, 1552−1562.
(28) Ma, M. Q.; Zhang, C.; Chen, T. T.; Yang, J.; Wang, J. J.; Ji, J.; Xu, Z. K. Bioinspired polydopamine/polyzwitterion coatings for underwater anti-oil and -freezing surfaces. *Langmuir* **2019**, *35*, 1895−1901.
(29) Chang, Y.; Shih, Y. J.; Lai, C. J.; Kung, H. H.; Jiang, S. Y. Blood-inert surfaces via ion-pair anchoring of zwitterionic copolymer brushes in human whole blood. *Adv. Funct. Mater.* **2013**, *23*, 1100−1110.
(30) Sin, M. C.; Chen, S. H.; Chang, Y. Hemocompatibility of zwitterionic interfaces and membranes. *Polym. J.* **2014**, *46*, 436−443.
(31) Lin, S.; Li, Y.; Zhang, L.; Chen, S.; Hou, L. Zwitterion-like, charge-balanced ultrathin layers on polymeric membranes for antifouling property. *Environ. Sci. Technol.* **2018**, *52*, 4457−4463.
(32) Yang, R.; Xu, J.; Ozaydin-Ince, G.; Wong, S. Y.; Gleason, K. K. Surface-tethered zwitterionic ultrathin antifouling coatings on reverse osmosis membranes by initiated chemical vapor deposition. *Chem. Mater.* **2011**, *23*, 1263−1272.
(33) Yu, H.-Y.; Kang, Y.; Liu, Y.; Mi, B. Grafting polyzwitterions onto polyamide by click chemistry and nucleophilic substitution on nitrogen: A novel approach to enhance membrane fouling resistance. *J. Membr. Sci.* **2014**, *449*, 50−57.
(34) Bernstein, R.; Belfer, S.; Freger, V. Bacterial attachment to ro membranes surface-modified by concentration-polarization-enhanced graft polymerization. *Environ. Sci. Technol.* **2011**, *45*, 5973−5980.
(35) Chan, W.-F.; Chen, H.-y.; Surapathi, A.; Taylor, M. G.; Hao, X.; Marand, E.; Johnson, J. K. Zwitterion functionalized carbon nanotube/polyamide nanocomposite membranes for water desalination. *ACS Nano* **2013**, *7*, 5308−5319.
(36) Du, H. B.; Qian, X. H. The hydration properties of carboxybetaine zwitterion brushes. *J. Comput. Chem.* **2016**, *37*, 877−885.
(37) Nagumo, R.; Ito, T.; Akamatsu, K.; Miura, R.; Suzuki, A.; Tsuboi, H.; Hatakeyama, N.; Takaba, H.; Miyamoto, A. Molecular dynamics simulations for microscopic behavior of water molecules in the vicinity of zwitterionic self-assembled monolayers. *Polym. J.* **2012**, *44*, 1149−1153.
(38) Shao, Q.; He, Y.; Jiang, S. Y. Molecular dynamics simulation study of ion interactions with zwitterions. *J. Phys. Chem. B* **2011**, *115*, 8358−8363.
(39) Shao, Q.; He, Y.; White, A. D.; Jiang, S. Y. Difference in hydration between carboxybetaine and sulfobetaine. *J. Phys. Chem. B* **2010**, *114*, 16625−16631.
(40) Xiang, Y.; Xu, R. G.; Leng, Y. S. Molecular simulations of the hydration behavior of a zwitterion brush array and its antifouling property in an aqueous environment. *Langmuir* **2018**, *34*, 2245−2257.
(41) Jorgensen, W. L.; Maxwell, D. S.; TiradoRives, J. Development and testing of the opls all-atom force field on conformational energetics and properties of organic liquids. *J. Am. Chem. Soc.* **1996**, *118*, 11225−11236.
(42) Kaminski, G. A.; Friesner, R. A.; Tirado-Rives, J.; Jorgensen, W. L. Evaluation and reparametrization of the opls-aa force field for proteins via comparison with accurate quantum chemical calculations on peptides. *J. Phys. Chem. B* **2001**, *105*, 6474−6487.
(43) Breneman, C. M.; Wiberg, K. B. Determining atom-centered monopoles from molecular electrostatic potentials - the need for high sampling density in formamide conformational-analysis. *J. Comput. Chem.* **1990**, *11*, 361−373.
(44) Shao, Q.; Jiang, S. Y. Effect of carbon spacer length on zwitterionic carboxybetaines. *J. Phys. Chem. B* **2013**, *117*, 1357−1366.
(45) Berendsen, H. J. C.; Postma, J. P. M.; van Gunsteren, W. F.; Hermans, J. *Interaction Models for Water in Relation to Protein Hydration*; D. Riedel Publishing Co.: Dordrecht, The Netherlands, 1981.
(46) Teleman, O.; Jonsson, B.; Engstrom, S. A molecular dynamics simulation of a water model with intramolecular degrees of freedom. *Mol. Phys.* **1987**, *60*, 193−203.
(47) Aqvist, J. Ion water interaction potentials derived from free-energy perturbation simulations. *J. Phys. Chem. A.* **1990**, *94*, 8021−8024.
(48) Joung, I. S.; Cheatham, T. E., 3rd Determination of alkali and halide monovalent ion parameters for use in explicitly solvated biomolecular simulations. *J. Phys. Chem. B* **2008**, *112*, 9020−9041.
(49) Plimpton, S. Fast parallel algorithms for short range molecular dynamics. *J. Comput. Phys.* **1995**, *117*, 1−19.
(50) Hockney, R. W.; Eastwood, J. W. *Computer Simulation Using Particles*; Taylor and Francis Group: London, U.K., 1988.
(51) Allen, M. P.; Tildesley, D. J. *Computer Simulation of Liquids*; Clarendon Press: Oxford, 1987.
(52) Kumar, S.; Bouzida, D.; Swendsen, R. H.; Kollman, P. A.; Rosenberg, J. M. The weighted histogram analysis method for free-energy calculations on biomolecules. I. The method. *J. Comput. Chem.* **1992**, *13*, 1011−1021.
(53) Torrie, G. M.; Valleau, J. P. Nonphysical sampling distributions in monte carlo free-energy estimation: Umbrella sampling. *J. Comput. Phys.* **1977**, *23*, 187−199.
(54) Gröger, G.; Stepanenko, V.; Würthner, F.; Schmuck, C. Step-wise self-assembly of a small molecule with two orthogonal binding interactions leads to single stranded linear polymers in DMSO. *Chem. Commun.* **2009**, 698−700.
(55) Rehm, T. H.; Schmuck, C. Ion-pair induced self-assembly in aqueous solvents. *Chem. Soc. Rev.* **2010**, *39*, 3597−3611.
(56) Rodler, F.; Linders, J.; Fenske, T.; Rehm, T.; Mayer, C.; Schmuck, C. pH-switchable vesicles from a serine-derived guanidiniocarbonyl pyrrole carboxylate zwitterion in DMSO. *Angew. Chem., Int. Ed.* **2010**, *49*, 8747−8750.
(57) Rybtchinski, B. Adaptive supramolecular nanomaterials based on strong noncovalent interactions. *ACS Nano* **2011**, *5*, 6791−6818.
(58) Schmuck, C.; Wienand, W. Highly stable self-assembly in water: Ion pair driven dimerization of a guanidiniocarbonyl pyrrole carboxylate zwitterion. *J. Am. Chem. Soc.* **2003**, *125*, 452−459.
(59) Bonomi, M.; Branduardi, D.; Bussi, G.; Camilloni, C.; Provasi, D.; Raiteri, P.; Donadio, D.; Marinelli, F.; Pietrucci, F.; Broglia, R. A.; Parrinello, M. Plumed: A portable plugin for free-energy calculations with molecular dynamics. *Comput. Phys. Commun.* **2009**, *180*, 1961−1972.
(60) Hummer, G.; Pratt, L. R.; Garcia, A. E. Free energy of ionic hydration. *J. Phys. Chem. B.* **1996**, *100*, 1206−1215.
(61) Chen, H. Y.; Ruckenstein, E. Hydrated ions: From individual ions to ion pairs to ion clusters. *J. Phys. Chem. B* **2015**, *119*, 12671−12676.
(62) Carrillo-Tripp, M.; Saint-Martin, H.; Ortega-Blake, I. A comparative study of the hydration of na+ and k+ with refined polarizable model potentials. *J. Chem. Phys.* **2003**, *118*, 7062−7073.
(63) Rowley, C. N.; Roux, B. The solvation structure of na+ and k+ in liquid water determined from high level ab initio molecular dynamics simulations. *J. Chem. Theory Comput.* **2012**, *8*, 3526−3535.
(64) Xiang, Y.; Liu, Y. L.; Mi, B. X.; Leng, Y. S. Hydrated polyamide membrane and its interaction with alginate: A molecular dynamics study. *Langmuir* **2013**, *29*, 11600−11608.
(65) Xiang, Y.; Liu, Y. L.; Mi, B. X.; Leng, Y. S. Molecular dynamics simulations of polyamide membrane, calcium alginate gel, and their interactions in aqueous solution. *Langmuir* **2014**, *30*, 9098−9106.
(66) Zhao, W. Q.; Zhu, Y. N.; Zhang, J. M.; Xu, T.; Li, Q. S.; Guo, H. S.; Zhang, J. W.; Lin, C. G.; Zhang, L. A comprehensive study and comparison of four types of zwitterionic hydrogels. *J. Mater. Sci.* **2018**, *53*, 13813−13825.
(67) Xue, W.; Huglin, M. B.; Liao, B. Observations on the swelling characteristics of the zwitterionic hydrogel of poly(1-3-sulfopropyl)-2-vinyl-pyridinium-betaine hydrogel. *Eur. Polym. J.* **2006**, *42*, 3015−3023.
(68) de Grooth, J.; Ogieglo, W.; de Vos, W. M.; Gironès, M.; Nijmeijer, K.; Benes, N. E. Swelling dynamics of zwitterionic

https://dx.doi.org/10.1021/acs.langmuir.0c01287
Langmuir XXXX, XXX, XXX−XXX

839 copolymers: The effects of concentration and type of anion and
840 cation. *Eur. Polym. J.* **2014**, *55*, 57−65.
841 (69) Kobayashi, M.; Ishihara, K.; Takahara, A. Neutron reflectivity
842 study of the swollen structure of polyzwitterion and polyeletrolyte
843 brushes in aqueous solutione. *J. Biomater. Sci., Polym. Ed.* **2014**, *25*,
844 1673−1686.
845 (70) Yang, Z. F.; Zhang, S. W.; Tarabara, V. V.; Bruening, M. L.
846 Aqueous swelling of zwitterionic poly(sulfobetaine methacrylate)
847 brushes in the presence of ionic surfactants. *Macromolecules* **2018**, *51*,
848 1161−1171.
849 (71) Lee, W. F.; Tsai, C. C. Synthesis and solubility of the
850 poly(sulfobetaine)s and the corresponding cationic polymers .2.
851 Aqueous-solution properties of poly n,n′-dimethyl(acrylamido
852 propyl) ammonium propane sulfonate. *Polymer* **1995**, *36*, 357−364.
853 (72) Marcus, Y. Effect of ions on the structure of water: Structure
854 making and breaking. *Chem. Rev.* **2009**, *109*, 1346−1370.
855 (73) Birkner, M.; Ulbricht, M. Ultrafiltration membranes with
856 markedly different ph- and ion-responsivity by photografted
857 zwitterionic polysulfobetain or polycarbobetain. *J. Membr. Sci.* **2015**,
858 *494*, 57−67.
859 (74) Xiang, T.; Luo, C.-D.; Wang, R.; Han, Z.-Y.; Sun, S.-D.; Zhao,
860 C.-S. Ionic-strength-sensitive polyethersulfone membrane with
861 improved anti-fouling property modified by zwitterionic polymer via
862 in situ cross-linked polymerization. *J. Membr. Sci.* **2015**, *476*, 234−
863 242.
864 (75) Mi, L.; Giarmarco, M. M.; Shao, Q.; Jiang, S. Divalent cation-
865 mediated polysaccharide interactions with zwitterionic surfaces.
866 *Biomaterials* **2012**, *33*, 2001−2006.

https://dx.doi.org/10.1021/acs.langmuir.0c01287
Langmuir XXXX, XXX, XXX−XXX